South African Journal of Chemical Engineering 58 (2026) 100968

Contents lists available at ScienceDirect

South African Journal of Chemical Engineering

journal homepage: www.elsevier.com/locate/sajce

The influence of various training algorithms on the effectiveness of thermal conductivity prediction for MgO-GO/water–ethylene glycol hybrid nanofluid: A more effective method for network training

Narinderjit Singh Sawaran Singh [a], Waleed Alaloosi [b], Muntadher Abed Hussein [c], Ali Abdul Karim Qasim [d], Dheyaa J. Jasim [e], Laith S. Sabri [f], Albara Ibrahim Alrawashdeh [g,h], Mahmut Taner [i], Soheil Salahshour [j,k,l,m,*], S. Ali Eftekhari [n,*]

[a] Faculty of Data Science and Information Technology, INTI International University, Persiaran Perdana BBN, Putra Nilai, Nilai 71800, Malaysia
[b] Department of Medical Instruments Engineering Techniques, College of Engineering, University of Al Maarif, Al Anbar,31001, Iraq
[c] University of Manara, Amarah, Maysan, Iraq
[d] Department of Mechanical Power Technical Engineering, Al-Amarah University College, Maysan, Iraq
[e] College of Engineering, University of Al Maarif, Al Anbar,31001, Iraq
[f] College of Chemical Engineering, University of Technology, Baghdad, 10066, Iraq
[g] Department of General Subjects, College of Engineering, University of Business and Technology, Jeddah 21361, Saudi Arabia
[h] Department of Chemistry and Chemical Technology, College of Science, Tafila Technical University, Tafila 66110, Jordan
[i] Faculty of Engineering and Architecture, Istanbul Gelisim University, Istanbul, Türkiye
[j] Faculty of Engineering and Natural Sciences, Istanbul Okan University, Istanbul, Turkey
[k] Faculty of Engineering and Natural Sciences, Bahcesehir University, Istanbul, Turkey
[l] Research Center of Applied Mathematics, Khazar University, Baku, Azerbaijan
[m] Faculty of Science and Letters, Piri Reis University, Tuzla, Istanbul, Turkey
[n] Department of Mechanical Engineering, Kho.C., Islamic Azad University, Khomeinishahr, Iran

ARTICLE INFO

Keywords:
Training algorithms
Performance
Thermal conductivity prediction
Hybrid nanofluid
Graphene oxide
Energy conservation

ABSTRACT

Accurate prediction of the thermal conductivity of hybrid nanofluids is essential for the design and optimization of advanced thermal management systems. In the present study, an artificial neural network framework was developed to predict the thermal conductivity of magnesium oxide–graphene oxide/water–ethylene glycol hybrid nanofluids using experimentally measured data. A total of 45 experimental datasets were generated by varying the temperature from 20 to 60 °C and the nanoparticle volume fraction from 0 to 0.20 vol.%. A feed-forward multilayer perceptron network was constructed, and ten backpropagation training algorithms were systematically evaluated to identify the optimum predictive model. Among the investigated algorithms, the Levenberg–Marquardt algorithm exhibited the highest predictive performance, achieving a mean squared error of 1.976×10^{-6}, a root mean square error of 1.395×10^{-3} W/m·K, a correlation coefficient of 0.9965, and a coefficient of determination of 0.9920. The robustness and generalization capability of the developed model were further confirmed through regression analysis, residual analysis, and 5-fold cross-validation, which yielded root mean square errors ranging from 8.38×10^{-4} to 4.73×10^{-3} W/m·K. A comparison with support vector regression, random forest, and Gaussian process regression demonstrated that the proposed model achieved highly competitive predictive accuracy while maintaining stable performance across different validation datasets. Furthermore, global Sobol sensitivity analysis identified nanoparticle volume fraction as the dominant governing parameter, whereas temperature exerted a considerably smaller influence on thermal conductivity. The observed enhancement in thermal conductivity was primarily attributed to the formation of conductive particle networks and improved interfacial heat transport associated with increasing nanoparticle loading. The

Abbreviations: ANN, Artificial Neural Network; GO, Graphene oxide; EG, Ethylene Glycol; HNF, Hybrid Nanofluid; φ, Volume Fraction; TC, Thermal Conductivity; MgO, Magnesium Oxide; NP, Nanoparticle; T, Temperature; MSE, Mean Squared Error; FF, Feed Forward; MP, Multilayer perceptron; ED, Experimental Datasets; H_2O, Water.

* Corresponding authors.
E-mail addresses: narinderjits.sawaran@newinti.edu.my (N.S.S. Singh), soheil.salahshour1361@gmail.com (S. Salahshour), a.eftekhari@iaukhsh.ac.ir (S. Ali Eftekhari).

https://doi.org/10.1016/j.sajce.2026.100968
Received 2 July 2026; Received in revised form 18 July 2026; Accepted 8 August 2026
Available online 9 August 2026

proposed framework provided an accurate, robust, and computationally efficient methodology for predicting the thermophysical behavior of hybrid nanofluids and can be readily extended to estimate other thermophysical properties using appropriate experimental datasets.

1. Introduction

Conventional heat transfer fluids, such as water (H_2O), ethylene glycol (EG), and their mixtures are widely used in cooling, heating, and energy conversion systems; however, their relatively low thermal conductivity (TC) limits their ability to satisfy the increasing thermal management demands of advanced engineering applications (Lenert et al., 2012).To overcome this limitation, nanofluids (NF) have been introduced as engineered suspensions in which solid nanoparticles (NPs) are dispersed within a base fluid to improve heat transfer performance (Ghanbarpour et al., 2014). The addition of NPs can enhance the effective TC of the working fluid by intensifying energy transport at the solid–liquid interface and creating additional conductive pathways within the fluid medium. Among different NP families, metal oxide NPs have attracted considerable attention because of their chemical stability, relatively simple synthesis procedure, lower production cost, and improved suspension stability compared with many metallic NPs (Wen et al., 2009; Hentschke, 2016; Jamshidi et al., 2012). In recent years, hybrid nanofluids (HNFs) have attracted substantial interest because combining multiple NPs can provide superior thermophysical performance compared with conventional single-particle NFs.Despite these advantages, the TC of NFs is influenced by several coupled parameters, including NP volume fraction (φ), temperature (T), particle morphology, and base fluid composition. Consequently, developing accurate predictive models for TC remains challenging when conventional empirical correlations are used outside their limited experimental ranges. Although experimental measurements provide reliable results, they are often time-consuming, expensive, and restricted to specific operating conditions (Chen et al.; Kang et al., 2009). Therefore, robust, data-driven modeling approaches are required to estimate NF thermal behavior with high accuracy and reduced experimental effort. Over the past decade, intelligent computational techniques, such as genetic algorithms (GA), fuzzy logic systems, adaptive neuro-fuzzy inference systems, and artificial neural networks (ANN), have increasingly been utilized to model complex nonlinear engineering systems (Stockwell, 1999; Dutt-Mazumder et al., 2011; Matthews and Swatman; Keskin et al., 2006; Takassi et al., 2011)). Among these methods, ANNs have demonstrated remarkable capability for learning nonlinear relationships directly from experimental datasets (ED) without requiring explicit mathematical formulations (Soleymani et al., 2011).

Recent studies demonstrated that ANNs can effectively model the nonlinear thermophysical behavior of NFs under different operating conditions. Most early investigations primarily focused on predicting single thermophysical properties, particularly TC and viscosity. For example, Akhgar et al. (2019) developed ANN models for estimating the TC of MWCNT–TiO_2/H_2O–EG-HNFs and reported close agreement between predicted and experimental values. Similarly, Hemmat Esfe et al. (2014) employed ANN techniques for Magnesium oxide (MgO)/EG-NF and demonstrated that ANN-based predictions could accurately reproduce TC trends across different operating conditions. These studies confirmed that ANN methods were highly effective for capturing nonlinear variations in TC, especially in hybrid and oxide-based NF systems. In addition to TC prediction, several researchers extended ANN applications toward viscosity estimation and thermal-fluid behavior analysis. Toghraie et al. (2019) predicted the viscosity of Ag/EG-NFs at different Ts and NP- φs and reported that ANN models achieved higher accuracy than conventional empirical correlations. Faridzadeh et al. (2014) further applied ANN methods to analyze mixed convection behavior in Cu/H_2O-NF-filled cavities, indicating that ANN models were capable of reproducing complex thermal-flow interactions in convective systems. Compared with direct thermophysical property prediction, these studies involved more complicated transport phenomena and demonstrated the flexibility of ANN approaches in handling multidimensional thermal systems.ANN techniques were utilized in broader thermal engineering and physicochemical applications. Hakeem et al. (2008) investigated T profile prediction in thermosyphon reboilers and achieved prediction errors lower than 3.4%, while Shanbedi et al. (2013)ccessfully estimated the thermal performance of CNT-based thermosyphon systems using ANN methods. Moreover, Jafari et al. (2015) demonstrated that ANN approaches were not limited to heat transfer applications alone and can also accurately predict thermodynamic behavior in electrolyte-containing systems. More recent investigations by Rostami et al. (2021) and He et al. (2020) focused on HNFs with enhanced thermal characteristics and confirmed that ANN models can successfully capture the coupled effects of T and NP-φ on TC behavior. Collectively, these studies indicated that ANN techniques provided robust and flexible frameworks for modeling complex nonlinear behavior across a wide range of HF and thermal engineering applications. Marulasiddeshi et al. (2022) investigated the thermophysical properties of H_2O-based Al_2O_3 and Al_2O_3–CuO-HNFs over different Ts and NP- φ s. Their results showed that the HNF provided greater enhancements in TC and viscosity than the mono NF while maintaining good suspension stability. Furthermore, empirical correlations and a cascaded forward neural network model were developed to accurately predict the thermophysical properties, demonstrating the potential of HNFs for advanced thermal management and solar energy applications. Akilu et al. (2024) experimentally investigated the heat transfer and friction characteristics of EG- and glycerol-based SiO_2-NFs flowing through a circular tube under constant heat flux conditions. Their results demonstrated that NP addition increased the heat transfer coefficient, though an increase in the friction factor accompanied it. Furthermore, several machine learning models were developed to predict thermohydraulic performance, with decision trees, random forests, and extreme gradient boosting achieving high predictive accuracy. Sharma et al. (2025) investigated the heat transfer performance of SiO_2-NFs dispersed in an H_2O–glycerol base fluid. Their results showed that NP addition enhanced the convective heat transfer coefficient while slightly increasing the friction factor. The authors further developed XGBoost and multi-gene genetic programming (MGGP) models to predict the thermohydraulic behavior, with the XGBoost model demonstrating superior predictive performance. Kanti et al. (2024); Kanti et al. (2025a); Kanti et al. (2025b) conducted a series of studies on the thermophysical characterization and machine learning-based prediction of NFs and HNFs for advanced thermal management applications. Their investigations demonstrated that NP- φ, T, and base fluid composition play dominant roles in determining TC, viscosity, and overall heat transfer performance. Experimental results consistently showed that graphene oxide(GO) and reduced GO-based NFs exhibited superior TC enhancements, whereas increasing the EG content generally increased viscosity while reducing TC. In addition to thermophysical property evaluation, the authors examined the thermohydraulic behavior of Al_2O_3/CuO-HNFs under turbulent flow conditions, reporting substantial improvements in heat transfer accompanied by a reduction of up to 71% in total entropy generation compared with pure H_2O. To accurately predict thermophysical and thermohydraulic characteristics, various machine learning approaches, including deep neural networks, linear regression, decision trees, and extreme gradient boosting (XGBoost), were developed and compared. Among these models, XGBoost consistently demonstrated the highest predictive accuracy for TC, viscosity, Nusselt number, friction factor, and entropy generation.

Despite considerable progress in ANN- and machine-learning-based prediction of NF thermophysical properties, several important research gaps remain. Most previous studies primarily focused on developing a single predictive model or comparing different machine learning algorithms to improve prediction accuracy, whereas the influence of ANN architecture, hidden-layer configuration, activation functions, and training algorithms on model performance received limited attention. Moreover, no systematic investigation has been reported to optimize the ANN training strategy for MgO–GO/H_2O–EG-HNFs, despite their highly nonlinear thermophysical behavior. To address these limitations, the present study developed an ANN-based predictive framework for TC prediction using experimentally measured data obtained under different Ts and NP-φs. Unlike previous investigations, the proposed framework systematically evaluated different network architectures, hidden neuron configurations, activation functions, and ten widely used ANN training algorithms under identical training conditions to identify the most accurate and computationally efficient predictive model. In addition to comparing prediction accuracy, the investigated algorithms were assessed for convergence behavior, regression performance, computational efficiency, and robustness across repeated independent training runs. Consequently, the present study provided not only an optimized ANN model for MgO–GO/H_2O–EG-HNFs but also a comprehensive assessment of ANN training strategies, serving as a practical guideline for developing reliable data-driven models for complex thermophysical systems.

2. Method of experiment

In the present study, EDs were generated to investigate the effects of T and NP-φ on the TC of MgO–GO/H_2O–EG-HNFs. The HNF was prepared using a two-step method at different NP-φ of 0, 0.03, 0.05, 0.10, and 0.20 vol.%. Ultrasonication was employed during preparation to improve NP dispersion and reduce particle agglomeration in the base fluid. The experimental T range was varied from 20 to 60 °C to evaluate the TC behavior under different operating conditions. The selected T and NP- φ ranges were adopted based on previously reported experimental investigations on MgO–GO/H_2O–EG-HNFs to ensure acceptable suspension stability and reliable TC measurements under practical operating conditions (Roohani and Toghraie, 2022). The TC of prepared HNFs was experimentally measured using a KD2-Pro thermal properties analyzer equipped with a KS1 probe based on the transient hot-wire technique. A total of 45 ED points were obtained by combining five NP-φs with nine T conditions (20, 25, 30, 35, 40, 45, 50, 55, and 60 °C) ((Roohani and Toghraie, 2022). These EDs were subsequently used to develop, train, and evaluate ANN models. Finally, different ANN configurations were examined to assess the influence of training algorithms and network architecture on TC prediction accuracy for MgO–GO/H_2O–EG-HNFs.

2.1. The NFs preparation

The MgO–GO/H_2O–EG-HNF was prepared using a two-step method. In this procedure, MgO-NPs and GO-NPs were dispersed into an H_2O–EG base fluid to prepare HNFs with different NP-φs. The base fluid consisted of a homogeneous mixture of distilled H_2O and EG. Initially, the required amount of NPs was gradually added to the base fluid under continuous magnetic stirring to improve the preliminary dispersion of NPs within the liquid medium. Subsequently, ultrasonication was employed to enhance suspension stability and minimize NP agglomeration. The prepared mixtures were sonicated using an ultrasonic device for a specific duration under controlled operating conditions to obtain a more uniform NP distribution. The ultrasonication process improved intermolecular interactions between NPs and the base fluid while reducing particle clustering within the suspension. Different NP-φs of 0.03, 0.05, 0.10, and 0.20 vol.% were prepared to investigate the influence of φ on the TC behavior of HNF. The stability of the prepared HNFs was visually monitored after preparation, and no significant sedimentation was observed during the experimental measurements. The prepared samples were then used for TC measurements at Ts ranging from 20 to 60 °C.

2.2. TC measurement

The TC of prepared MgO–GO/H_2O–EG-HNFs was measured experimentally using a KD2-Pro thermal properties analyzer equipped with a KS1 single-needle sensor, based on the transient hot-wire method. Before each measurement, the NF samples were maintained at the desired T in a controlled-T environment to ensure thermal equilibrium throughout the measurement.TC measurements were conducted at temperatures of 20, 25, 30, 35, 40, 45, 50, 55, and 60 °C for different NP-φs. To improve measurement reliability and minimize random experimental fluctuations, each test was repeated several times under identical operating conditions, and the average value was reported as the final TC. During the experiments, the KS1 probe was fully immersed in the NF sample to ensure stable thermal contact between the sensor and the fluid medium. The transient hot-wire technique was selected because of its high accuracy and suitability for TC measurements of NFs and low-viscosity liquid systems. The obtained experimental TC data were subsequently used as the input dataset for ANN modeling and prediction analysis.

2.3. Measurement repeatability and uncertainty analysis

To improve the reliability of experimental measurements, the TC of each sample was measured several times under identical operating conditions, and the average value was reported as the final result. The averaged TC values were subsequently used as input to the ANN; therefore, repeated measurements were not treated as independent training samples. Before each experiment, the KD2-Pro thermal properties analyzer was calibrated according to the manufacturer's recommended procedure to ensure consistent and stable measurements. Measurement uncertainty was evaluated through repeated experiments, instrument accuracy checks, and comparisons with reference data. The measured TC of base fluid showed excellent agreement with the ASHRAE standard, with a maximum measurement error of only 0.1%, confirming the high accuracy and repeatability of the experimental procedure (Handbook-Fundamentals, 2009). This low measurement uncertainty indicated that the ED used for ANN development was reliable and suitable for predictive modeling.

3. The ANN

ANNs were powerful computational tools capable of modeling complex nonlinear relationships between input and output variables. Owing to their high approximation capabilities, they were widely used to predict the thermophysical properties of NFs (Braspenning, 1995).

Fig. 1 presents the overall workflow adopted in the present investigation. Initially, TC data were experimentally measured at different Ts and NP- φs. The ED was subsequently preprocessed and randomly divided into training, validation, and testing subsets for ANN development. Various network architectures and training algorithms were systematically evaluated to identify the optimal predictive model. The selected ANN was then validated through regression analysis, residual analysis, and five-fold cross-validation to assess its predictive accuracy and generalization capability. Finally, Sobol sensitivity analysis was performed to quantify the relative influence of the input variables, and the predictive performance of the developed ANN was benchmarked against support vector regression (SVR), random forest (RF), and Gaussian process regression (GPR).

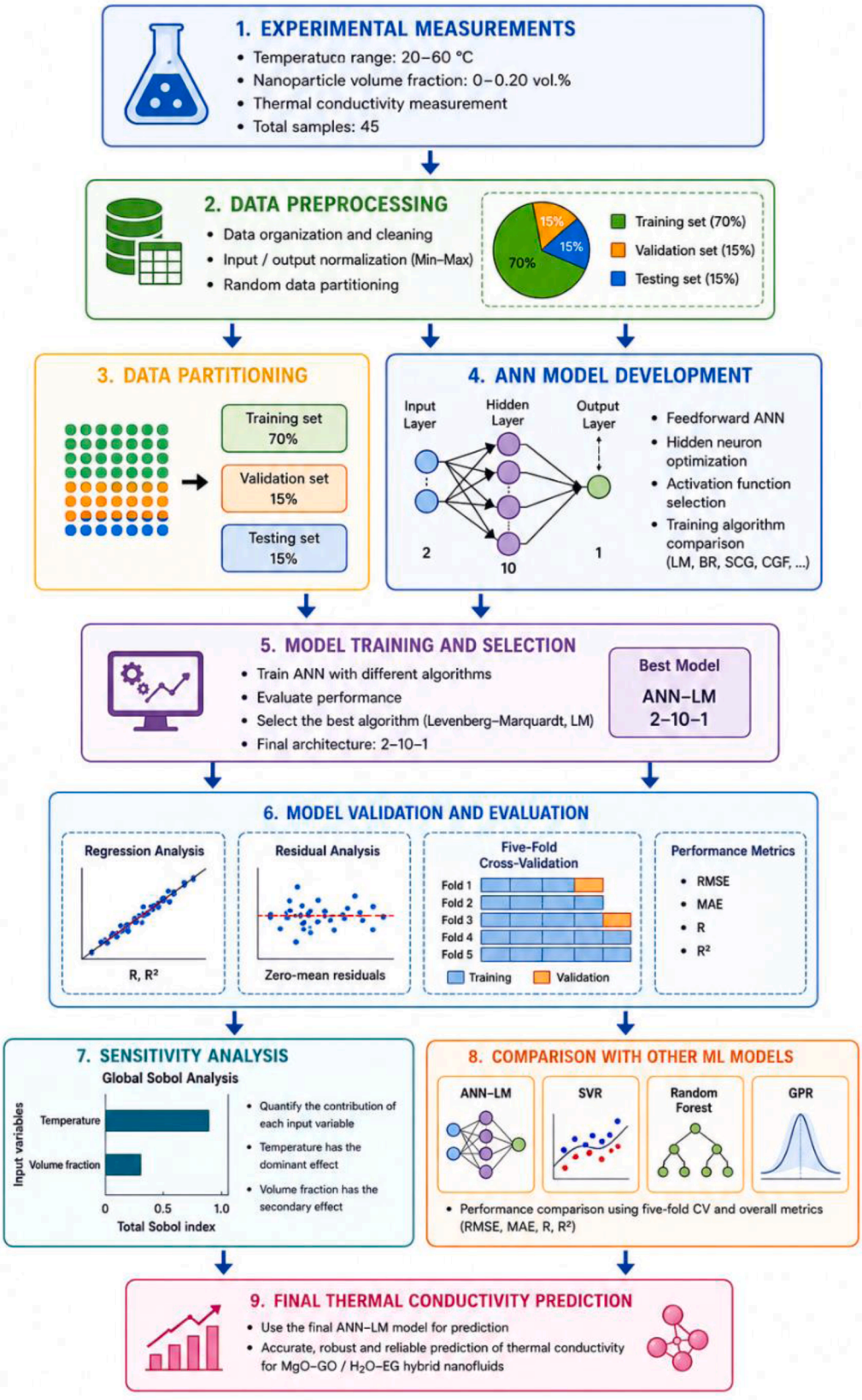

Fig. 1. Overall workflow of the proposed methodology for TC prediction of MgO–GO/H_2O–EG-HNFs.

3.1. Configuration

In the present study, a feedforward multilayer perceptron (FFMLP) architecture was employed to establish the relationship between the input variables and the TC of MgO–GO/H_2O–EG-HNFs. The network consisted of two input neurons corresponding to T and NP-φ, and one output neuron representing TC. Before the training process, the input and output variables were normalized using the mapminmax preprocessing function available in MATLAB. This normalization transformed all variables into the same numerical range, thereby improving numerical stability during training, accelerating convergence, and preventing variables with different magnitudes from disproportionately influencing the optimization process. The ANN models were developed using 45 experimentally measured TC data reported by Roohani and Toghraie (2022). These data comprised five NP-φ (0, 0.03, 0.05, 0.10, and 0.20 vol.%) evaluated at nine Ts ranging from 20 to 60 °C. To develop and evaluate the ANN models, the dataset was randomly split into three subsets: 70% for training, 15% for validation, and 15% for testing. This data partitioning strategy provided a suitable balance between parameter optimization and independent model evaluation, while maintaining sufficient training samples despite the relatively limited size of ED. The validation subset was used to monitor network performance during training and to reduce the risk of overfitting via an early-stopping strategy, whereas the testing subset was used exclusively for the final assessment of model generalization.

Network training was performed using MATLAB's built-in early stopping strategy. The stopping conditions included a maximum of 200 training epochs, a performance goal of 1×10^{-8}, and a maximum of six consecutive validation failures (max_fail = 6). Training was automatically terminated once the target performance was reached or when no further improvement in the validation error was observed for six consecutive validation checks. This approach prevented overfitting while ensuring stable convergence and robust generalization of the developed ANN model. Different ANN configurations were examined by varying the number of hidden neurons and evaluating different activation functions. The network architecture with the lowest prediction error and the highest regression accuracy was selected as the optimal model. Among the examined configurations, the best predictive performance was achieved with a single hidden layer containing 10 neurons and a hyperbolic tangent sigmoid (tansig) activation function, with a linear (purelin) transfer function in the output layer to predict continuous TC values. The selected architecture provided an appropriate compromise between prediction accuracy and network complexity. The network parameters were optimized using supervised backpropagation learning, and ten commonly used training algorithms available in MATLAB were comparatively evaluated under identical network architecture and data partitioning conditions. Their predictive performance was assessed using several statistical indicators, including mean squared error (MSE), root mean squared error (RMSE), mean absolute error (MAE), coefficient of determination (R^2), and correlation coefficient (R). Among the evaluated algorithms, the Levenberg–Marquardt (trainlm) algorithm exhibited the highest prediction accuracy and was therefore selected as the optimal training algorithm for the present investigation. Training was performed using MATLAB's default early-stopping procedure, which continuously monitored the validation error during the optimization. Training was automatically terminated when no further improvement in validation performance was observed, thereby preventing unnecessary iterations and reducing the likelihood of overfitting. The final ANN model was intended for interpolation within the investigated experimental domain, corresponding to Ts between 20 and 60 °C and NP-φ between 0 and 0.20 vol.%. Consequently, predictions outside these experimental ranges should be interpreted with caution because experimental observations did not support them. Fig. 2 illustrates the architecture of the employed FFMLP network, including the input, hidden, and output layers, while the experimental TC dataset used for ANN development and performance evaluation is summarized in Table 1.

The deviation of TC and its range based on different Ts and φs are presented in Figs. 3 and 4, respectively.

Following the architecture optimization process, the configuration that provided the best compromise between prediction accuracy and network complexity was selected as the final ANN model. The adopted network consisted of a single hidden layer with ten neurons, employing the hyperbolic tangent sigmoid (tansig) transfer function, while the output layer used a linear (purelin) transfer function to predict continuous TC values. The complete configuration parameters of the selected ANN model are summarized in Table 2.

Table 1
TC versus T with different φ.

T	φ (%)				
(°C)	0	0.03	0.05	0.10	0.20
20	0.532	0.546	0.557	0.568	0.576
25	0.534	0.548	0.557	0.569	0.577
30	0.535	0.551	0.558	0.57	0.58
35	0.536	0.553	0.559	0.572	0.583
40	0.536	0.555	0.561	0.575	0.588
45	0.538	0.557	0.563	0.576	0.588
50	0.54	0.559	0.564	0.577	0.589
55	0.541	0.56	0.565	0.579	0.59
60	0.542	0.561	0.566	0.58	0.59

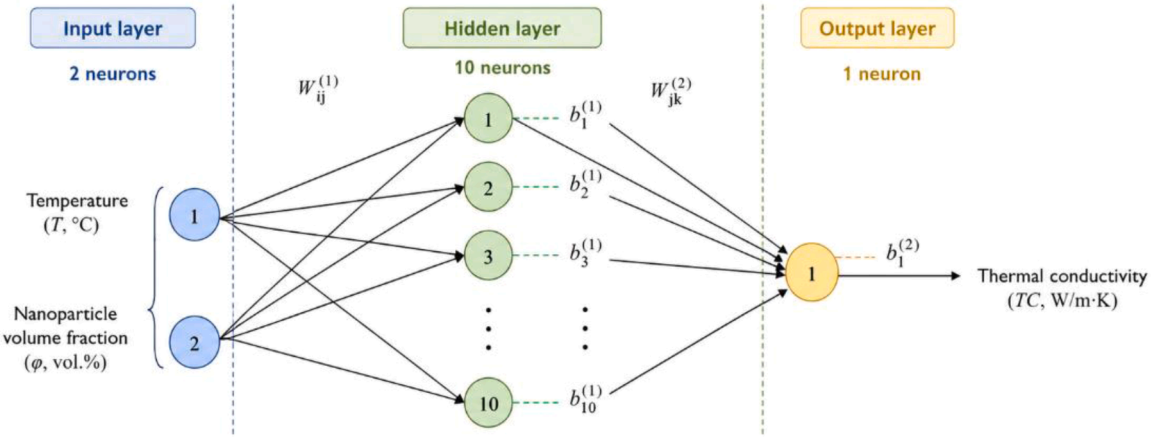

Fig. 2. Schematic representation of an MLP-ANN showing the structure of input and output variables.

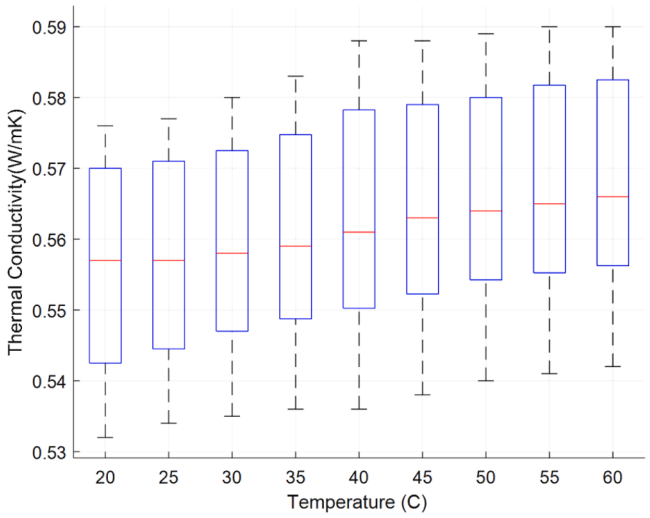

Fig. 3. TC deviation based on T.

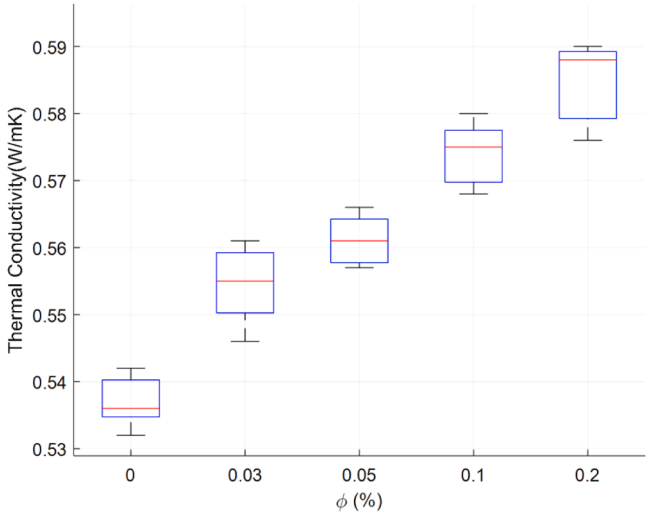

Fig. 4. TC variation due to φ.

Table 2
The ANN configuration.

Network Parameter	Information
ANN construction	(MP)
ANN type	(FF)
Training Method	(Back Propagation)
Error Criteria	MSE
Best Training Method	Trainlm
Number of Hidden Layers	1
Hidden Layer function	tansig, logsig
Output Layer function	Purelin
Number of Training Data	29
Number of Validation Data	6–7
Number of Test Data	6–7

3.2. Training methods

A key objective of the present investigation was to identify the most reliable ANN training algorithm for predicting the TC of MgO–GO/H_2O–EG-HNFs. To achieve this objective, ten supervised back-propagation training algorithms available in MATLAB were systematically evaluated under identical conditions, including the same FFMLP architecture, network configuration, data partitioning strategy, and preprocessing procedure (MacKay, 1992; Foresee and Hagan; Powell, 1977; Murray et al., 2019; Møller, 1993; Riedmiller and Braun). Such a unified framework ensured that the observed differences in predictive performance originated solely from the optimization characteristics of the training algorithms, rather than from variations in network architecture or dataset allocation. Furthermore, to reduce the influence of random weight and bias initialization, each training algorithm was independently executed 30 times with different random initializations, and the average performance indicator values were subsequently calculated. The predictive capability of each training algorithm was quantitatively assessed using the MSE, RMSE, R, R^2, and computational training time. These complementary statistical indicators enabled a comprehensive evaluation of prediction accuracy, regression quality, computational efficiency, and model robustness, thereby providing a more reliable basis for algorithm selection than reliance on a single error metric. The quantitative performance metrics for all investigated training algorithms are summarized in Table 3, and the corresponding MSE comparisons are presented in Fig. 5 to provide a clear visualization of their relative prediction accuracy.

As summarized in Table 3, the Levenberg–Marquardt (LM) algorithm exhibited the best overall performance, producing the lowest prediction errors and the highest values of the correlation coefficient and coefficient of determination. These results demonstrate the LM algorithm's superior ability to capture the nonlinear relationships among T, NP-φ, and TC, with high predictive accuracy. Although several alternative algorithms also produced satisfactory predictions, their comparatively larger error values and lower regression statistics indicate reduced predictive capability under identical training conditions. Based on the combined criteria of prediction accuracy, regression performance, robustness, and computational efficiency, the LM algorithm was selected for subsequent analyses. Its predictive performance was further investigated through regression analysis and performance curves to provide additional validation of the developed ANN model. To further verify the robustness and generalization capability of the selected LM model, a five-fold cross-validation analysis was conducted using the complete ED. In this validation procedure, the available data were randomly partitioned into five approximately equal subsets: four for model training and one for independent testing. This process was repeated five times so that each sample was used once for validation and four times for training. As illustrated in Fig. 6, the RMSE values remained consistently low throughout the cross-validation process, ranging from 0.00,084 to 0.00,473 W/m·K, with an average of 0.00,243 W/m·K. The relatively narrow variation in prediction error among the five validation folds indicates that the developed ANN maintained a stable level of predictive accuracy despite changes in the training and testing partitions. The narrow range of RMSE values across the five validation folds confirms the stability of the developed ANN when different subsets of the ED are used for training and validation. The absence of substantial variations in prediction error indicates that the model maintained consistent predictive performance throughout cross-validation, thereby providing independent verification of its robustness and generalization capability. These findings further support the reliability of the proposed ANN for predicting the TC of MgO–GO/H_2O–EG-HNFs within the investigated T and NP-φ ranges.

3.3. Comparison with alternative ML models

To provide an independent benchmark for the developed ANN, its predictive performance was compared with support vector regression (SVR), random forest (RF), and Gaussian process regression (GPR). All models were evaluated using the same five-fold cross-validation partitions to ensure a consistent and unbiased comparison. The predictive performance was assessed using the mean fold RMSE, the standard deviation of RMSE, the out-of-fold RMSE, the out-of-fold MAE, R, and R^2. The corresponding results are summarized in Table 4. Among the investigated models, GPR achieved the lowest out-of-fold RMSE and

Table 3
Comparison of the performance of different ANN training algorithms based on the average results of 30 independent training runs.

Acronym	AL	MSE	RMSE	R	R^2	Training time (s)
BR	trainbr	5.963×10^{-6}	1.955×10^{-3}	0.99,099	0.97,590	0.0770
LM	trainlm	1.976×10^{-6}	1.395×10^{-3}	0.99,653	0.99,201	0.0817
CGB	traincgb	4.012×10^{-5}	4.370×10^{-3}	0.96,439	0.83,783	0.0811
CGF	traincgf	4.652×10^{-5}	4.867×10^{-3}	0.95,923	0.81,195	0.0869
CGP	traincgp	4.699×10^{-5}	5.067×10^{-3}	0.95,507	0.81,007	0.0769
RP	trainrp	4.891×10^{-5}	5.687×10^{-3}	0.92,745	0.80,230	0.0565
SCG	trainscg	6.358×10^{-5}	5.980×10^{-3}	0.92,400	0.74,301	0.0600
GDA	traingda	1.747×10^{-4}	1.217×10^{-2}	0.77,325	0.29,381	0.2026
BFG	trainbfg	2.322×10^{-4}	1.285×10^{-2}	0.81,310	0.06,129	0.0769
GDX	traingdx	2.955×10^{-4}	1.520×10^{-2}	0.69,691	−0.19,432	0.1728

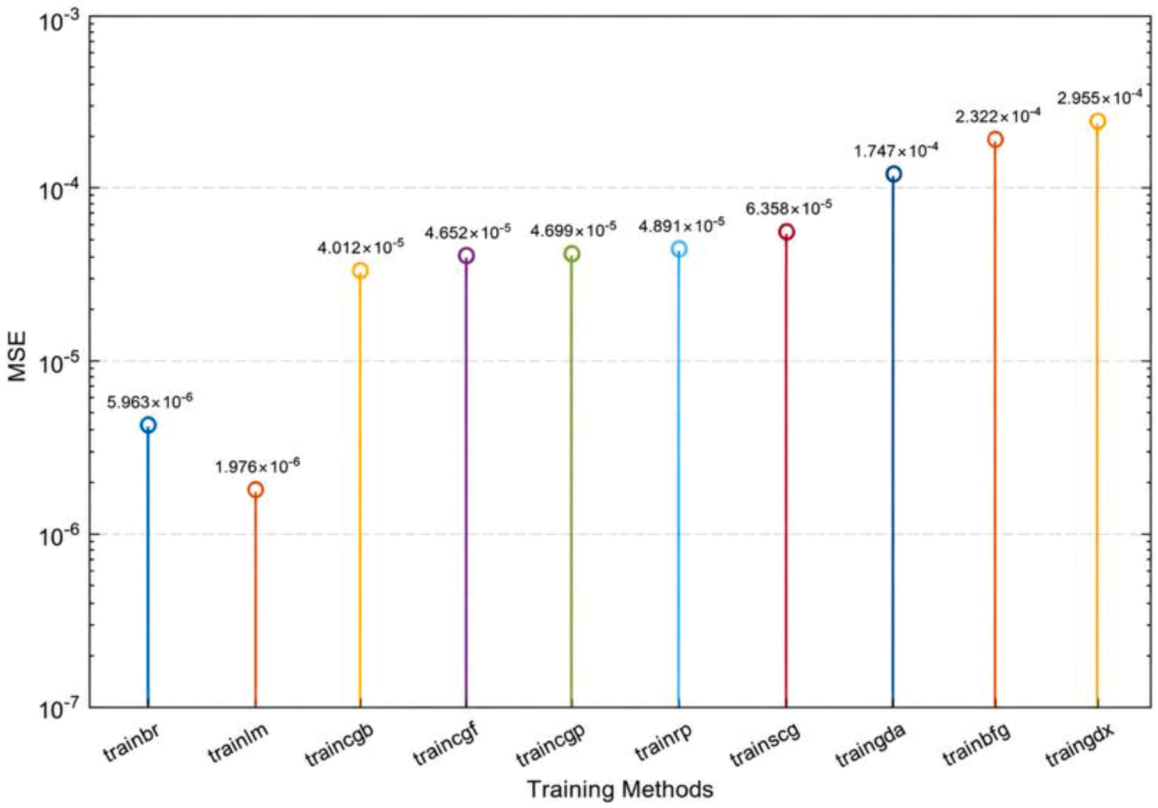

Fig. 5. Comparison of the prediction accuracy of different ANN training algorithms based on the MSE obtained from 30 independent training runs for TC prediction of MgO–GO/H_2O–EG-HNFs.

MAE values of 0.001,421 W/m·K and 0.001,181 W/m·K, respectively, together with the highest out-of-fold R^2 of 0.99,290. The ANN-LM model exhibited performance closely comparable to the baseline, with an out-of-fold RMSE of 0.001,488 W/m·K, an MAE of 0.001,232 W/m·K, and an R^2 of 0.99,222. Although the average GPR RMSE was marginally lower, the ANN-LM model had the smallest standard deviation in fold-specific RMSE values, indicating greater consistency across training and test partitions.

In contrast, SVR exhibited moderately higher prediction errors, whereas RF showed the lowest predictive accuracy, with an out-of-fold RMSE of 0.005,857 W/m·K and an R^2 of 0.87,938. The close agreement between the ANN-LM and GPR results demonstrated that both nonlinear modeling approaches accurately represented the relationships among T, NP-φ, and TC. However, the lower variation in ANN performance across the validation folds indicated that the developed ANN maintained more stable predictive accuracy across data partitions. Therefore, although GPR provided a marginal improvement in the overall error indices, the ANN-LM model remained highly competitive and offered a reliable framework for TC prediction within the investigated experimental domain.

3.4. Trained ANN performance

The training process was systematically monitored using a performance plot that showed the MSE as a function of the number of training epochs. Fig. 7 illustrates this performance trajectory for the ANN developed to predict the TC of GO/H_2O–EG HNF. The MSE values for the training, validation, and test datasets were displayed simultaneously, enabling a comprehensive evaluation of the model's learning behavior and generalization capacity. At the initial stages of training, the network parameters were randomly initialized, resulting in relatively high MSE values. As training proceeded, these values declined as the network weights were iteratively optimized. The early stopping technique was employed to terminate training when the validation error began to increase, thereby preventing overfitting and ensuring reliable performance on unseen data. This optimal stopping point, indicated in Fig. 7, corresponds to the epoch with the lowest validation error and reflects the best balance between underfitting and overfitting. Among 50

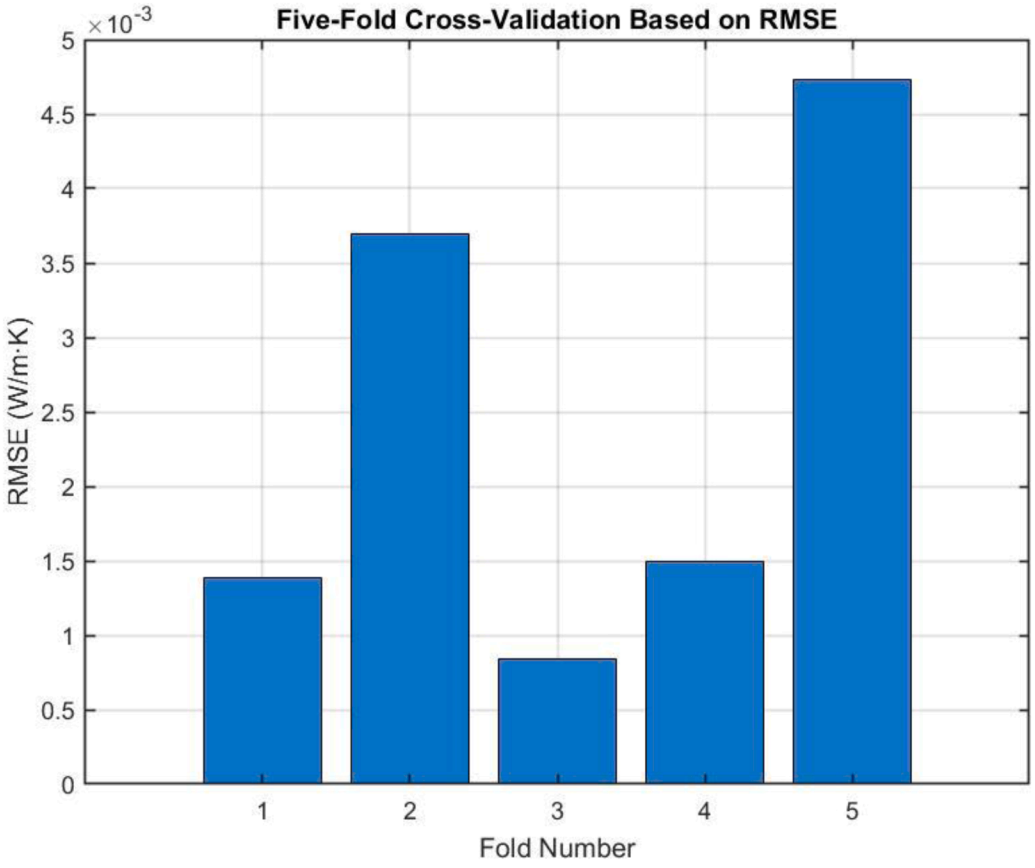

Fig. 6. Five-fold cross-validation results expressed in terms of RMSE for the developed ANN model.

Table 4
Five-fold cross-validated performance comparison of the ANN-LM, SVR, RF, and GPR models for TC prediction.

Model	Mean fold RMSE (W/m·K)	SD of RMSE (W/m·K)	OOF RMSE (W/m·K)	OOF MAE (W/m·K)	OOF R	OOF R^2
ANN-LM	0.001,473	0.000,235	0.001,488	0.001,232	0.99,657	0.99,222
SVR	0.002,065	0.000,899	0.002,216	0.001,587	0.99,241	0.98,274
Random forest	0.005,645	0.001,748	0.005,857	0.004,607	0.97,669	0.87,938
GPR	0.001,378	0.000,388	0.001,421	0.001,181	0.99,656	0.99,290

distinct ANN configurations trained under identical conditions, the model with the lowest validation error at this optimal epoch was selected as the most accurate and robust for predicting TC across various combinations of input parameters. This systematic approach to model selection enhanced confidence in the predictive reliability of the final network architecture.

The predictive capability of the developed ANN was further evaluated through regression analysis by comparing predicted TC values with corresponding experimental measurements. As illustrated in Fig. 8, strong linear agreement was observed across the training, validation, and test datasets, indicating that the developed network accurately reproduced the experimental TC over the investigated operating range. To provide a more rigorous assessment of model performance, both R and R^2 were calculated separately for each data subset, and the corresponding results are summarized in Table 5. The obtained R values exceeded 0.9985, while the corresponding R^2 values remained higher than 0.9965 for all data subsets. The close agreement among the training, validation, and testing statistics indicated that no appreciable degradation in predictive performance occurred when the model was evaluated using previously unseen data. Furthermore, the consistently high R and R^2 values across all subsets confirmed that the developed ANN achieved excellent predictive accuracy and maintained stable generalization throughout the learning and validation processes.

To further evaluate the predictive behavior of the developed ANN, a residual analysis was performed by examining the differences between the experimental and predicted TC values, as illustrated in Fig. 9. The residuals remained within a narrow range of -1.52×10^{-3} to 2.91×10^{-3} W/m·K, with an average residual of 1.32×10^{-4} W/m·K. Moreover, the residuals were distributed on both sides of the zero-error line, without any pronounced systematic trend across the investigated TC range. The absence of a consistent overprediction or underprediction pattern indicated that the developed ANN did not introduce a noticeable systematic prediction bias. Combined with the consistently high regression statistics across the training, validation, and test datasets, the residual analysis further confirmed the robustness and predictive reliability of the proposed ANN model under the investigated operating conditions.

Fig. 10 illustrates the error distribution of ED for TC. The graph showed a high frequency of errors within the zero range, indicating that the network was effectively trained and capable of providing accurate TC estimates.

Fig. 11 presents a histogram of the ANN's error values. The bar chart illustrated the frequency of errors within various error ranges, with the vertical axis representing error frequency and the horizontal axis indicating the corresponding error margins. A high frequency of near-zero errors indicated the network's accuracy, as smaller error values suggested the model was making precise predictions. The zero-error line,

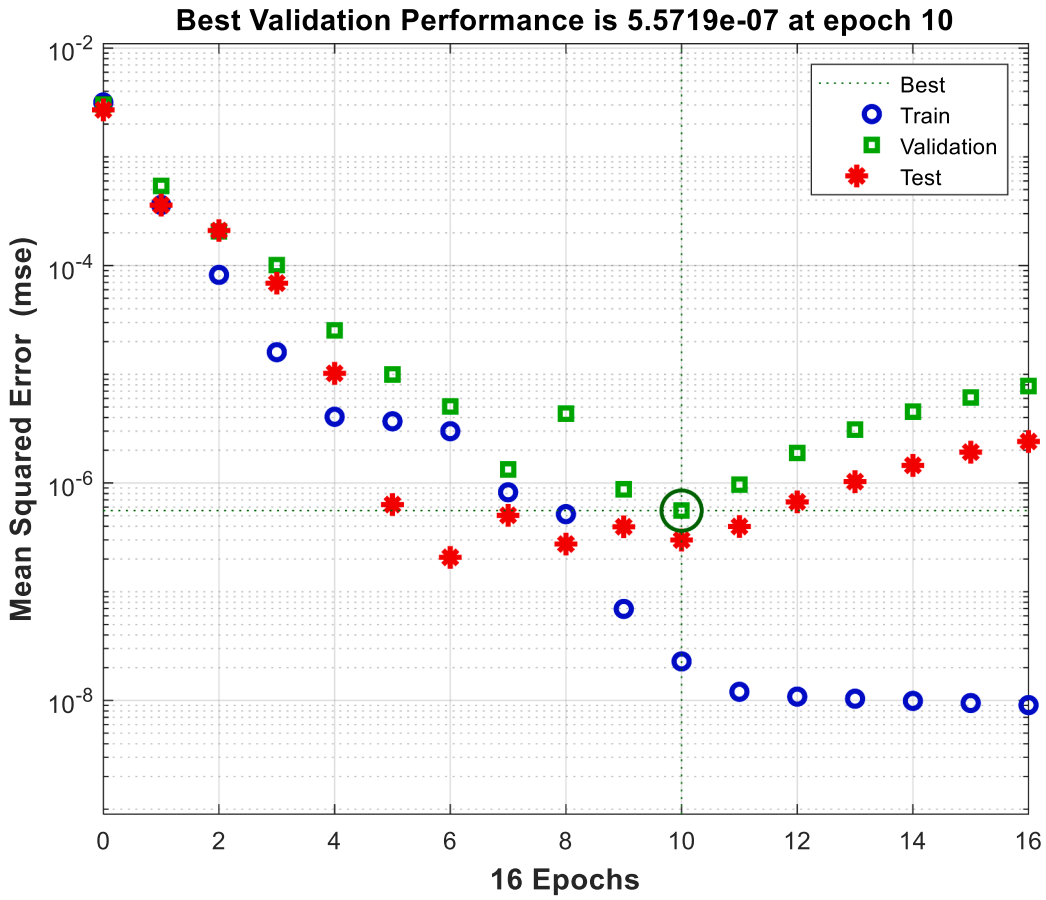

Fig. 7. ANN training performance curve based on the MSE.

marked in orange, highlighted the ideal point of perfect prediction. The majority of error values were concentrated around this line, confirming that the ANN's predictions were closely aligned with the target values. This distribution demonstrated the effectiveness of the training method. It suggested that the network was well-calibrated, producing accurate, reliable outputs with minimal deviation from the desired results.

Fig. 12 presents an additional comparison of ANN outputs and the target values. The results showed a good agreement between the ANN outputs and the target values, indicating that ANN training was appropriate.

3.5. Analyzing untrained data

To evaluate the trained ANN's performance in predicting previously unseen data, a three-dimensional comparison plot was presented in Fig. 13, showing the relationships among TC, T, and φ. In this visualization, the network's predictions for untrained data points were represented by a colored mesh, while the trained data points were marked with blue stars. The alignment of these stars with the 3D surface indicated a strong agreement between the predicted and target values for the untrained data, suggesting that the network effectively generalized to new inputs. Although minor local deviations may exist in limited regions of the prediction surface, the overall agreement between the predicted and target values for untrained datasets confirmed the acceptable generalization capability and stability of the developed ANN model within the investigated operating conditions. Upon reviewing the various graphical representations of trained ANNs' performance, it can be concluded that the model served as a reliable approximator for predicting TC. Additionally, the analysis revealed that φ had a more pronounced effect on TC than T, which exhibited a minimal influence on the output values. This indicated that the trained ANN can accurately predict TC based on φ, with T playing a negligible role in overall predictions.

Although the TC generally increased with both T and NP-φ, slight local deviations from a perfectly monotonic trend were observed at several intermediate NP-φs. Such behavior was characteristic of HNFs and may result from the combined effects of temporary NP agglomeration, particle-particle interactions, Brownian motion, and local variations in dispersion uniformity, all of which can locally modify heat transport pathways within the suspension. Nevertheless, the overall TC enhancement was predominantly driven by NP-φ. Increasing the NP loading led to a greater number of highly conductive MgO-NPs and GO nanosheets in the base fluid, thereby reducing the average interparticle distance and promoting the formation of continuous thermally conductive networks. In addition, the large specific surface area of GO enhanced solid-liquid interfacial contact, facilitating phonon transport across the interface and improving energy transfer throughout the suspension. By comparison, increasing T primarily intensified Brownian motion and localized micro-convective effects, which contributed to TC enhancement but to a considerably smaller extent than the formation of concentration-dependent conductive pathways within the investigated operating range. This physical interpretation was in excellent agreement with the global Sobol sensitivity analysis, which quantitatively identified NP-φ as the dominant governing variable, whereas T exhibited only a secondary contribution with relatively weak interaction effects. The consistency between the experimentally observed TC trends, the ANN predictions, and the global sensitivity analysis further demonstrated that the proposed data-driven framework successfully captured the underlying physical mechanisms controlling heat transport in MgO-GO/H_2O-EG-HNFs. Although the present investigation focused on TC, the developed modeling framework was not restricted to a single thermophysical property. Because the ANN architecture established nonlinear

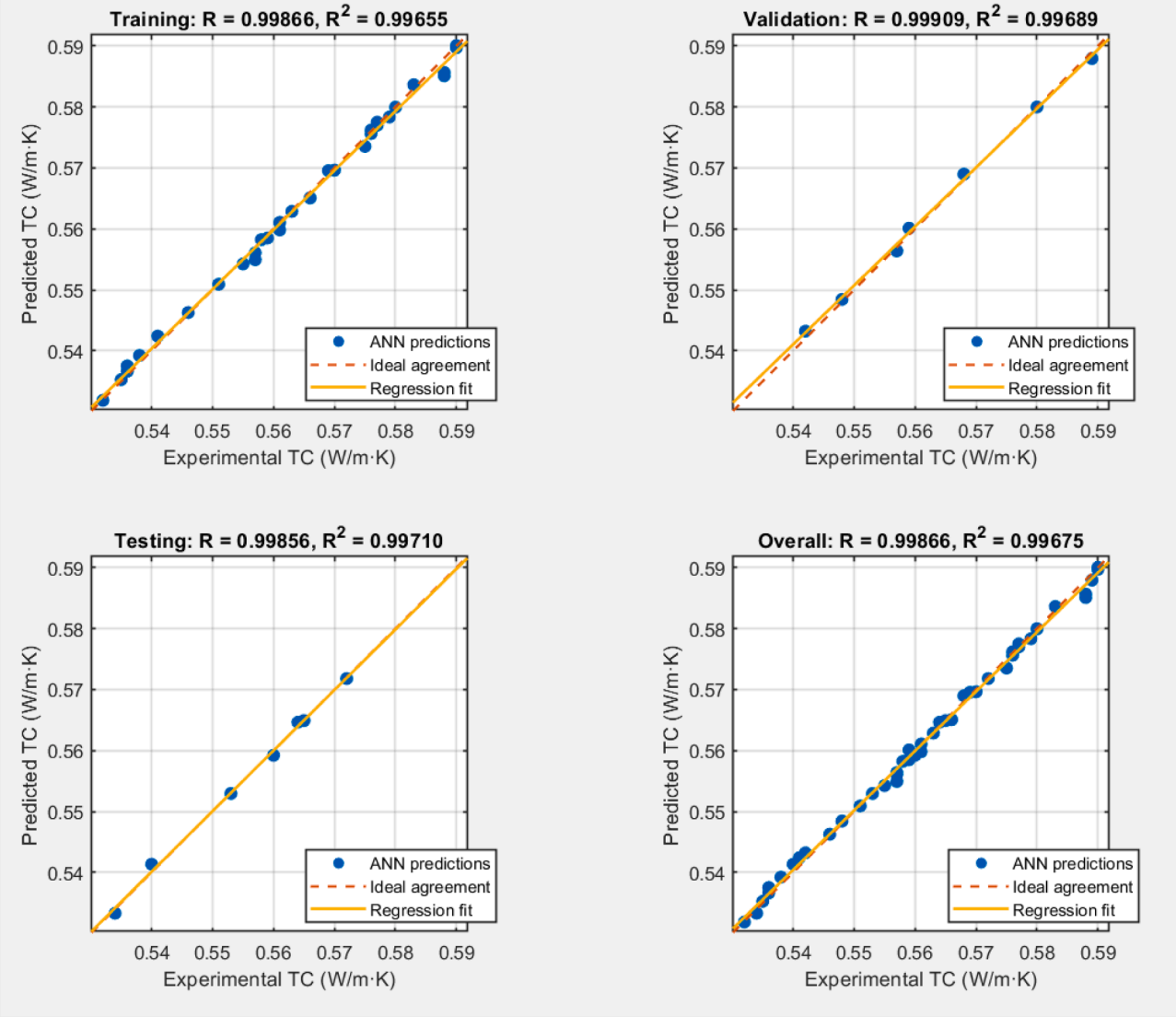

Fig. 8. Regression plots of the developed ANN for the training, validation, testing, and overall datasets.

Table 5
Regression statistics of the developed ANN model for the training, validation, testing, and overall datasets.

Dataset	R	R^2
Training	0.99,866	0.99,655
Validation	0.99,909	0.99,689
Testing	0.99,856	0.99,710
Overall	0.99,866	0.99,675

relationships between operating conditions and material responses without relying on property-specific governing equations, the same methodology can be readily extended to predict other thermophysical properties, including viscosity, density, specific heat capacity, and thermal diffusivity, provided that the corresponding EDs are available. Consequently, the proposed framework showed a versatile predictive platform for comprehensive thermophysical characterization, optimization, and design of advanced HNFs for thermal management applications.

3.6. Global Sobol sensitivity analysis

To quantitatively evaluate the relative influence of input variables on the predicted TC, a global Sobol sensitivity analysis was performed using the final ANN model. The first-order Sobol index (S_1) was employed to quantify the direct contribution of each input variable, whereas the total-order Sobol index (S_t) accounted for both the direct effect and its interactions with the remaining input variables. The corresponding sensitivity indices are summarized in Table 6. As shown in Table 6, NP-φ contributed most to the predicted TC, with first- and total-order Sobol indices of 0.8750 and 0.9067, respectively. In contrast, T showed considerably lower sensitivity, with corresponding S_1 and S_t values of 0.0941 and 0.1260. These results demonstrate that variations in NP-φ constituted the dominant factor governing the TC of investigated MgO–GO/H_2O–EG-HNF, whereas the influence of T was comparatively smaller within the investigated operating range. Furthermore, the relatively small differences between the first-order and total-order indices for both input variables (approximately 0.032) indicated that interaction effects between T and NP-φ are limited. This observation suggested that the ANN predictions were primarily governed by the independent contributions of input variables rather than by strong nonlinear interactions among them.

4. Conclusion

In this study, the effects of varying φ and Ts on the TC of MgO–GO/

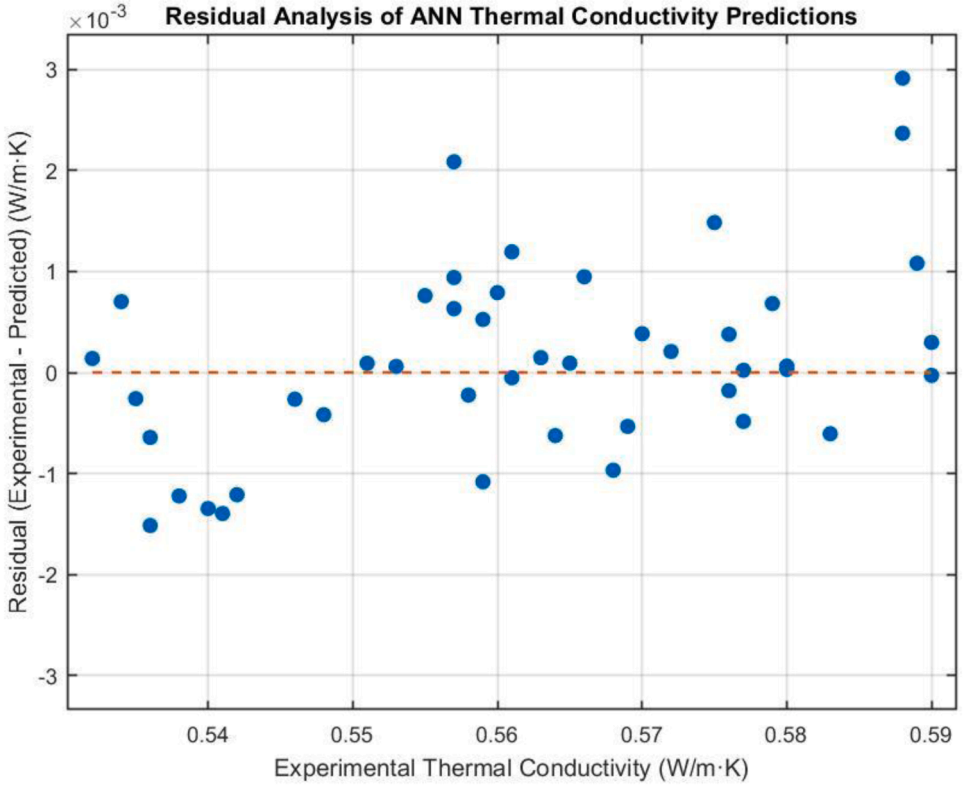

Fig. 9. Residual distribution between the experimental and ANN-predicted TC values over the investigated operating range.

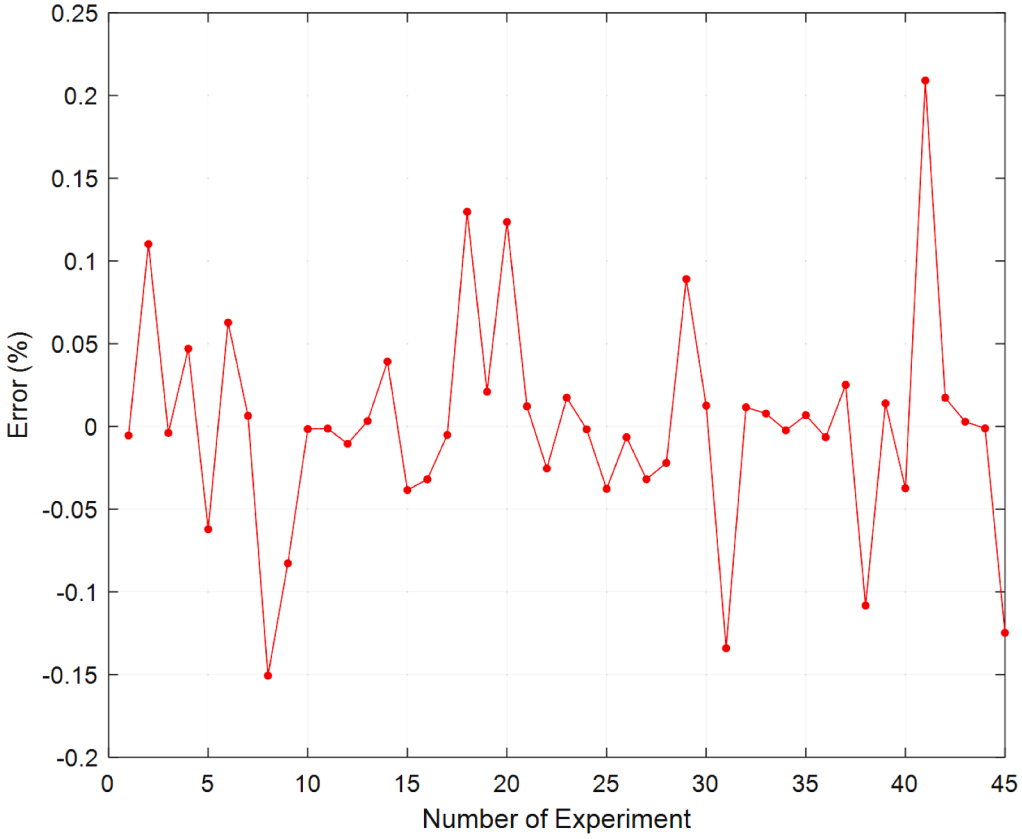

Fig. 10. Prediction ED of the developed ANN for TC.

H_2O–EG HNF were systematically analyzed. A total of 45 distinct experimental conditions were designed, incorporating five NP-φ values

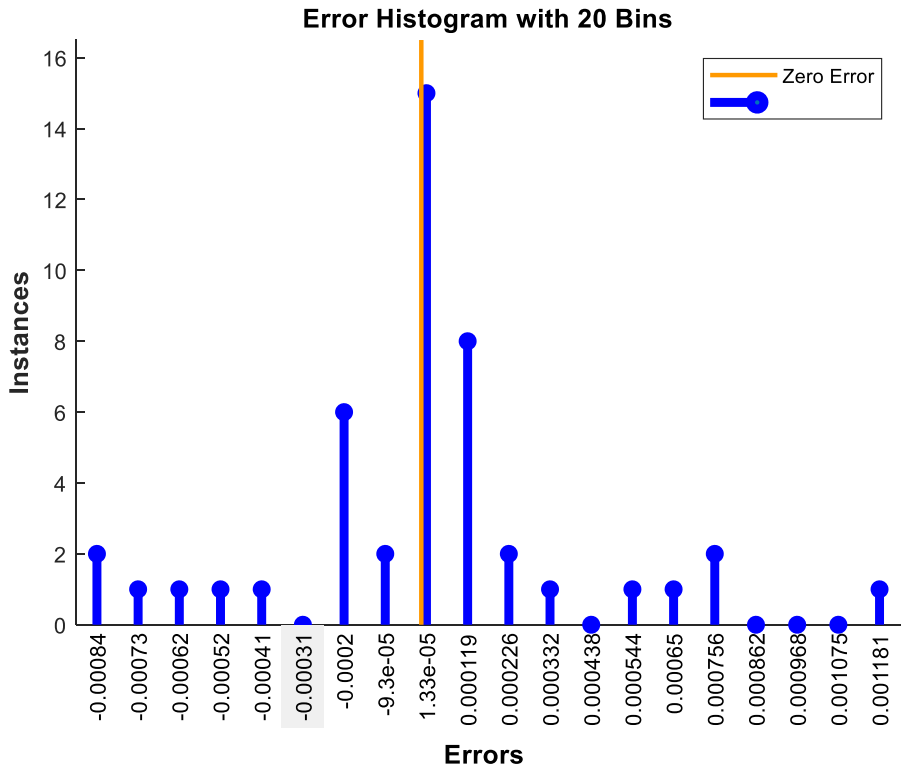

Fig. 11. Histogram of ANN prediction errors for TC.

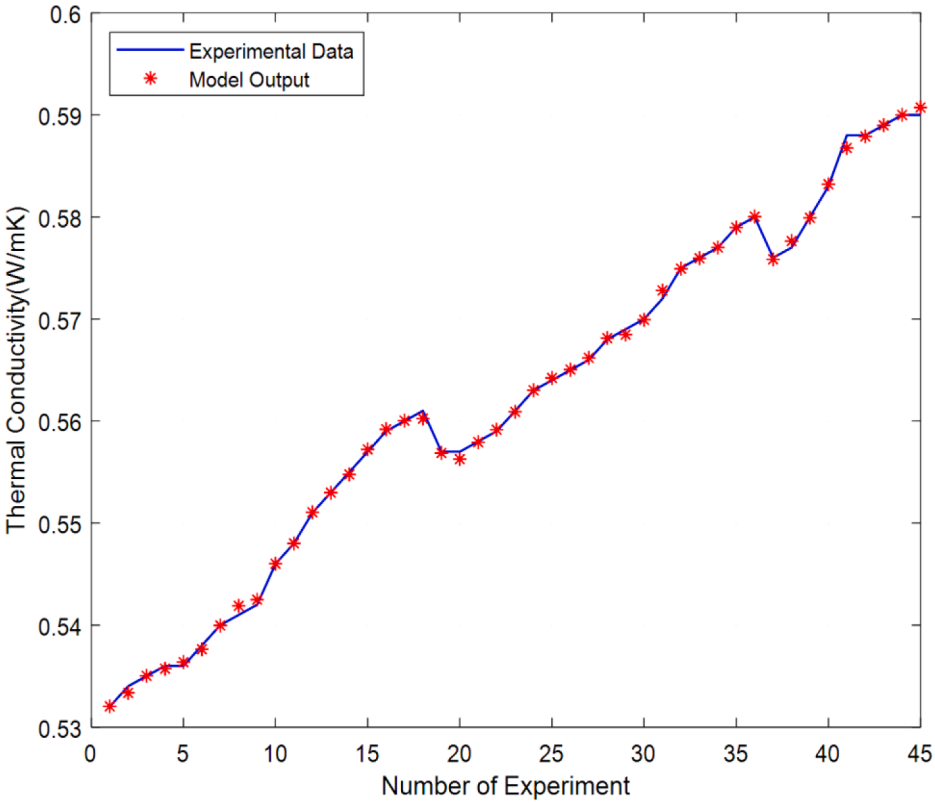

Fig. 12. Comparison between experimental and ANN-predicted TC values.

and nine T levels. These experimental results provided the necessary data to train an ANN capable of predicting the TC of NF within the defined input ranges of φ and T. The network architecture employed was an FF-MP ANN, with T and φ as input parameters and TC as the output. To enhance prediction accuracy, the network was trained using the Levenberg-Marquardt backpropagation algorithm (trainlm), which

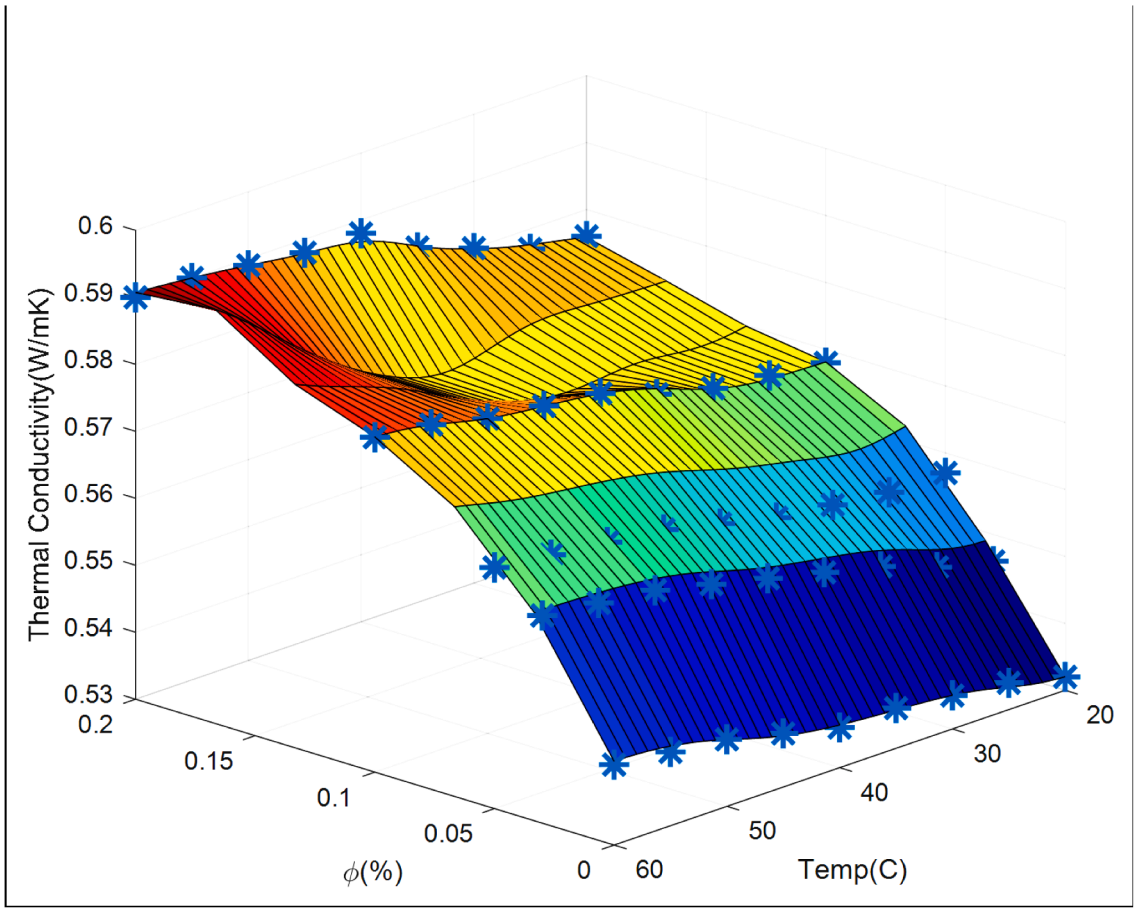

Fig. 13. 3D graph of TC versus T and φ.

Table 6
Global Sobol sensitivity indices of the developed ANN model for TC prediction.

Input variable	First-order index (S_1)	95% CI	Total-order index (S_t)	95% CI	$S_t - S_1$
NP- φ	0.8750	0.8732–0.8767	0.9067	0.8984–0.9152	0.0317
T	0.0941	0.0856–0.1026	0.1260	0.1243–0.1278	0.0319

yielded the highest performance among the training functions considered. The trained ANN was then used to predict k_{nf} for any given combination of input parameters. The summary of the obtained results is as follows:

- The TC of the MgO–GO/H_2O–EG-HNFs increased with both T and NP-φ.
- The maximum TC of 0.590 W/m·K was obtained at 60 °C and 0.20 vol.%, whereas the minimum value (0.532 W/m·K) corresponded to the base fluid at 20 °C, representing an overall enhancement of approximately 10.9% within the investigated operating range.
- Among the ten investigated backpropagation training algorithms, the LM (trainlm) algorithm achieved the best overall predictive performance, producing the lowest prediction errors with an MSE of 1.976×10^{-6} and an RMSE of 1.395×10^{-3} W/m·K, together with the highest regression accuracy, reaching an R value of 0.9965 and an R^2 value of 0.9920.
- The developed ANN demonstrated excellent predictive reliability, achieving R^2 values greater than 0.996 across the training, validation, and test datasets. Furthermore, five-fold cross-validation yielded RMSE values ranging from 8.38×10^{-4} to 4.73×10^{-3} W/m·K, confirming the robustness and generalization capability of the proposed model.
- Comparison with alternative machine learning techniques demonstrated that the developed ANN achieved predictive accuracy comparable to that of Gaussian process regression while providing more consistent performance across different validation folds and substantially outperforming support vector regression and random forest models.
- The experimental observations and global Sobol sensitivity analysis consistently identified NP-φ as the dominant factor controlling TC ($S_1 = 0.8750$), whereas T contributed considerably less ($S_1 = 0.0941$).

Although the developed ANN model demonstrated high predictive accuracy within the investigated operating conditions, the present framework was trained and evaluated using experimentally generated datasets within limited ranges of T and NP-φ. Therefore, validation with independent EDs and across broader operating conditions may further improve the generalization capability and applicability of the proposed predictive model for broader thermal engineering applications.

CRediT authorship contribution statement

Narinderjit Singh Sawaran Singh: Investigation, Funding acquisition, Writing – original draft, Writing – review & editing, Software, Validation, Conceptualization. **Waleed Alaloosi:** Investigation, Funding acquisition, Writing – original draft, Writing – review & editing, Software, Validation, Conceptualization. **Muntadher Abed Hussein:** Investigation, Funding acquisition, Writing – original draft, Writing – review & editing, Software, Validation, Conceptualization. **Ali Abdul**

Karim Qasim: Investigation, Funding acquisition, Writing – original draft, Writing – review & editing, Software, Validation, Conceptualization. **Dheyaa J. Jasim:** Investigation, Funding acquisition, Writing – original draft, Writing – review & editing, Software, Validation, Conceptualization. **Laith S. Sabri:** Investigation, Funding acquisition, Writing – original draft, Writing – review & editing, Software, Validation, Conceptualization. **Albara Ibrahim Alrawashdeh:** Investigation, Funding acquisition, Writing – original draft, Writing – review & editing, Software, Validation, Conceptualization. **Mahmut Taner:** Investigation, Funding acquisition, Writing – original draft, Writing – review & editing, Software, Validation, Conceptualization. **Soheil Salahshour:** Investigation, Funding acquisition, Writing – original draft, Writing – review & editing, Software, Validation, Conceptualization. **S. Ali Eftekhari:** Investigation.

Declaration of competing interests

The authors declare that they have no known competing financial interests or personal relationships that could have appeared to influence the work reported in this paper.

References

Akilu, S., Sharma, K., Baheta, A.T., Kanti, P.K., Paramasivam, P., 2024. Machine learning analysis of thermophysical and thermohydraulic properties in ethylene glycol-and glycerol-based SiO2 nanofluids. Sci. Rep. 14 (1), 14829.

A. Akhgar, D. Toghraie, N. Sina, and M. Afrand, "Developing dissimilar artificial neural networks (ANNs) to prediction the thermal conductivity of MWCNT-TiO2/Water-ethylene glycol hybrid nanofluid," vol. 355, pp. 602–610, 2019.

Braspenning, P.J., 1995. Artificial Neural networks: an Introduction to ANN Theory and Practice. Springer Science & Business Media.

Y.-T. Chen, W.-C. Wei, S.-W. Kang, and C.-S. Yu, "Effect of nanofluid on flat heat pipe thermal performance." pp. 16–19.

Dutt-Mazumder, A., Button, C., Robins, A., Bartlett, R., 2011. Neural network modelling and dynamical system theory: are they relevant to study the governing dynamics of association football players? Sports Med. 41, 1003–1017.

M. Faridzadeh, D.S. Toghraie, and A. Niroomand, "Analysis of laminar mixed convection in an inclined square lid-driven cavity with a nanofluid by using an artificial neural network," vol. 45, no. 4, 2014.

F.D. Foresee and M.T. Hagan, "Gauss-Newton approximation to Bayesian learning." pp. 1930–1935.

Ghanbarpour, M., Haghigi, E.B., Khodabandeh, R., 2014. Thermal properties and rheological behavior of water-based Al2O3 nanofluid as a heat transfer fluid. Exp. Therm. Fluid Sci. 53, 227–235.

M. Hakeem, M. Kamil, and I. Arman, "Prediction of temperature profiles using artificial neural networks in a vertical thermosiphon reboiler," vol. 28, no. 13, pp. 1572–1579, 2008.

A. Handbook-Fundamentals, "American Society of Heating, Refrigerating and Air-Conditioning Engineers", 2009.

He, W., Ruhani, B., Toghraie, D., Izadpanahi, N., Esfahani, N.N., Karimipour, A., Afrand, M., 2020. Using of artificial neural networks (ANNs) to predict the thermal conductivity of zinc oxide–silver (50%–50%)/water hybrid Newtonian nanofluid. Int. Commun. Heat Mass Transf. 116, 104645.

Hemmat Esfe, M., Saedodin, S., Bahiraei, M., Toghraie, D., Mahian, O., Wongwises, S., 2014. Thermal conductivity modeling of MgO/EG nanofluids using experimental data and artificial neural network. J. Therm. Anal. Calorim. 118, 287–294.

R. Hentschke, "On the specific heat capacity enhancement in nanofluids," vol. 11, pp. 1–11, 2016.

D. Jafari, S. Nowee, and I. Engineering, "Studies on the applicability of artificial neural network (ANN) in prediction of thermodynamic behavior of sodium chloride aqueous system containing a non-electrolytes," vol. 9, no. 1, pp. 110–113, 2015.

N. Jamshidi, M. Farhadi, D. Ganji, and K. Sedighi, "Experimental investigation on the viscosity of nanofluids," 2012.

S.-W. Kang, W.-C. Wei, S.-H. Tsai, and C. Huang, "Experimental investigation of nanofluids on sintered heat pipe thermal performance," vol. 29, no. 5-6, pp. 973–979, 2009.

Kanti, P.K., Sharma, P., Wanatasanappan, V.V., Said, N.M., 2024. Explainable machine learning techniques for hybrid nanofluids transport characteristics: an evaluation of shapley additive and local interpretable model-agnostic explanations. J. Therm. Anal. Calorim. 149 (21), 11599–11618.

Kanti, P.K., Marulasiddeshi, H., Said, N.M., Wanatasanappan, V., Paramasivam, P., Dabelo, L.H., 2025a. Bayesian-optimized machine learning and experimental study of al_2o_3-CuO hybrid nanofluid thermal performance in turbulent circular tube flow. Sci. Rep. 15 (1), 38717.

Kanti, P.K., H.G, P.K., Said, N.M., Wanatasanappan, V., Paramasivam, P., Dabelo, L.H., 2025b. Optimizing base fluid composition for PEMFC cooling: a machine learning approach to balance thermal and rheological performance. Sci. Rep. 15 (1), 27335.

Keskin, M.E., Taylan, D., Terzi, O., 2006. Adaptive neural-based fuzzy inference system (ANFIS) approach for modelling hydrological time series 51 (4), 588–598.

A. Lenert, Y. Nam, and E. Wang, "Heat transfer fluids," vol. 15, 2012.

D. MacKay, "Bayesian interpolation," vol. 4, no. 3, pp. 415–447, 1992.

Marulasiddeshi, H.B., Kanti, P.K., Jamei, M., Prakash, S.B., Sridhara, S.N., Said, Z., 2022. Experimental study on the thermal properties of Al2O3-CuO/water hybrid nanofluids: development of an artificial intelligence model. Int. J. Energy Res. 46 (15), 21066–21083.

C. Matthews, and P.A. Swatman, "Fuzzy concepts and formal methods: a fuzzy logic toolkit for z." pp. 491–510.

M. Møller, "A scaled conjugate gradient algorithm for fast supervised learning," vol. 6, no. 4, pp. 525–533, 1993.

W. Murray, M.H. Wright, and P.E. Gill, Practical optimization: SIAM-society for industrial and applied mathematics, 2019.

M. Powell, "Restart procedures for the conjugate gradient method," vol. 12, pp. 241–254, 1977.

M. Riedmiller and H. Braun, "A direct adaptive method for faster backpropagation learning: the RPROP algorithm." pp. 586–591.

Roohani, E., Toghraie, D., 2022. Heat transfer improvement of antifreeze by changing it to hybrid nanofluid: effects of hybrid magnesium oxide–graphene oxide nanopowders. J. Therm. Anal. Calorim. 147 (12), 6777–6791.

Rostami, S., Toghraie, D., Shabani, B., Sina, N., Barnoon, P., 2021. Measurement of the thermal conductivity of MWCNT-CuO/water hybrid nanofluid using artificial neural networks (ANNs). J. Therm. Anal. Calorim. 143 (2), 1097–1105.

Shanbedi, M., Jafari, D., Amiri, A., Heris, S.Z., Baniadam, M., 2013. Prediction of temperature performance of a two-phase closed thermosyphon using artificial neural network. Heat Mass Transf. 49, 65–73.

Sharma, K., Naik, M., Kanti, P.K., Prasad, D.R., Paramasivam, P., Ayanie, A.G., 2025. Flow and heat transfer of poly dispersed SiO2 nanoparticles in aqueous glycerol in a horizontal pipe: application of ensemble and evolutionary machine learning for model-prediction. PLoS One 20 (6), e0323347.

A.R. Soleymani, J. Saien, and H. Bayat, "Artificial neural networks developed for prediction of dye decolorization efficiency with UV/K2S2O8 process," vol. 170, no. 1, pp. 29–35, 2011.

D. Stockwell, "Genetic algorithms II: species distribution modelling," pp. 123–144, 1999.

M.A. Takassi, M.K. Salooki, and M. Esfandyari, "Fuzzy model prediction of Co (III) Al2O3 catalytic behavior in Fischer-Tropsch synthesis," vol. 20, no. 6, pp. 603–610, 2011.

Toghraie, D., Sina, N., Jolfaei, N.A., Hajian, M., Afrand, M., 2019. Designing an artificial neural network (ANN) to predict the viscosity of Silver/Ethylene glycol nanofluid at different temperatures and volume fraction of nanoparticles. Phys. A: Stat. Mech. Appl. 534, 122142.

D. Wen, G. Lin, S. Vafaei, and K. Zhang, "Review of nanofluids for heat transfer applications," vol. 7, no. 2, pp. 141–150, 2009.